Inverse optimization design of sugarcane seeding mechanism based on approximate multi-position and posture

Qingli Chen[1,2], Jiaodi Liu[1,2*], Hongzhen Xu[1,2], Yong Hua[1,2], Xiaoman Wu[1,2]

(1. *College of Mechanical and Control Engineering, Guilin University of Technology, Guilin 541004, Guangxi, China*;
2. *Key Laboratory of Advanced Manufacturing and Automation Technology (Guilin University of Technology), Education Department of Guangxi Zhuang Autonomous Region, Guilin 541006, Guangxi, China*)

Abstract: The current sugarcane seeding mechanism is unable to accomplish complex seeding movement trajectories and postures, thus failing to enable the cane seed to enter the seed trench in a stable posture, resulting in a high rate of collapse and a low survival rate. A second-order non-circular planetary gear system pendulum-type seeding mechanism is adopted to realize the complex motion of seeding arm taking seeds in an orderly manner, transporting seeds stably, and sowing seeds in a fixed posture. Constraining the position and posture of the end point of the seeding arm, based on the principle of second-order center distance invariance in the motion process of the planetary gear train, the inverse optimization design model of approximate multi-positional posture is established, and the initial optimal parameters of the double-motion point of the mechanism are solved by genetic algorithm. The second-order non-circular gear ratios are assigned according to the kinematic characteristics of the mechanism in order to design all the non-circular gear pitch curves and model their convexity calculations. In order to avoid the influence on the preset position and posture, the position of the corresponding relative angular displacement fitting point of the adjustable trajectory segment on the closed motion trajectory is taken as the optimization variable, and the convexity optimization model of the second-order non-circular gear pitch curve is established. A set of non-circular gear pitch curves with better roundness is obtained by *NSGA* II multi-objective optimization algorithm combined with entropy weight *TOPSIS* game theory. The simulation results show that the motion trajectory posture of the virtual prototype is basically consistent with the theoretical model, which meets the agronomic requirements of sugarcane seeding and verifies the feasibility of the mechanism design.

Keywords: sugarcane seeding, inverse optimization design, second-order non-circular planetary gear train, non-circular gear pitch curve convexity

DOI: 10.25165/j.ijabe.20251803.8797

Citation: Chen Q L, Liu J D, Xu H Z, Hua Y, Wu X M. Inverse optimization design of sugarcane seeding mechanism based on approximate multi-position and posture. Int J Agric & Biol Eng, 2025; 18(3): 73–81.

1 Introduction

Sugarcane seeding agronomy requires that the seed be dropped into the seed trench in a stable posture, with the axis of the seed parallel to the axis of the seed trench and the shoots facing the sides of the seed trench[1]. The traditional sugarcane seeder adopts the seed-dropping method of discharge tube, which has high seeding efficiency. However, due to the large height difference between the upper end of the seed discharge tube and the seed drop point, the cane seed slides for a long distance in the seed discharge tube and the trajectory and posture are unstable, with the result that the posture of the seed drop does not meet the agronomic requirements and the seed spacing cannot be maintained consistently. In order to solve the problem of sugarcane seeding that does not meet the agronomic requirements, it is necessary to ensure that the sugarcane seeding mechanism is able to hold the seed to complete the complex movement process of orderly seed picking, stable seed transportation, and fixed posture seeding. The posture of the seeds should also change periodically with the trajectory to ensure that the posture of the seeds and the seed spacing at the seed drop point are in accordance with the agronomic requirements.

The second-order non-circular gear pair is compact, smooth-running, and can constrain multiple degrees of freedom in space. Its unequal speed transmission characteristics can make the end point of the pendulum with the combination of the motion of the sub-part of the pendulum show a different periodic trajectory, while there are also a variety of pendulum postures, so it is widely used in transplanting or insertion machinery[2-4]. Nippon Inokan Agricultural Machinery Co., Ltd. was the first to utilize a combination of gears to realize the orderly transplanting of rice potting seedlings by a transplanting arm. However, the combination of spur gears used leads to the need for the mechanism to cooperate with the chute to complete the seedling picking action. In addition, the planting action depends on the duckbill transplanter with the transplanting arm to complete the transplanting action, which results in a complex and less efficient mechanism structure[5]. Yu et al.[6] used incomplete gears with a transplanting arm to realize the transplanting of rice potting seedlings, simplifying the overall complexity of the structure and effectively improving the transplanting success rate. Xu et al.[7] developed a fully automatic strawberry potting seedling transplanting machine, which not only meets the requirements of the strawberry potting seedling transplanting operation, but also

Received date: 2024-01-08 **Accepted date:** 2024-12-03

Biographies: **Qingli Chen**, MSc, research interest: intelligent agricultural machinery, Email: 2802574703@qq.com.com; **Hongzhen Xu**, PhD, Professor, research interest: intelligent agricultural machinery, Email: 514083869@qq.com; **Yong Hua**, MSc, research interest: intelligent agricultural machinery, Email: 1151766311@qq.com; **Xiaoman Wu**, MSc, research interest: intelligent agricultural machinery, Email: 2754659092@qq.com.

***Corresponding author: Jiaodi Liu**, PhD, research interest: intelligent agricultural machinery. College of Mechanical and Control Engineering, Guilin University of Technology, Guilin 541004, Guangxi, China. Tel: +86-13397836256, Email: timesea1572037232@163.com.

utilizes the non-circular gear pair to cooperate with the punching linkage to realize the periodic digging action and improve the overall transplanting efficiency. Liu et al.[8] controlled the periodic intermittent motion of second-order non-circular gears by means of end-face cams to obtain the ideal motion trajectory for transplanting operation, but the instant at which the cam-controlled gears disengage from the meshing is prone to rigid vibration. Zhou et al.[9] fitted the pitch curves of non-circular gears by Elmit interpolation to make the overall transplanting motion smoother. Sun et al.[10] used a multi-stage non-circular gear and multi-link combination drive to realize the integration of celery potting seedling picking up and planting. Although the structure of the mechanism is complex, the success rate of picking up the seedling is high and will not cause damage to the potting seedling in the process of transplanting. Mao et al.[11] used the parameter-guided heuristic optimization algorithm to optimize each structural parameter of the transplanting mechanism, overcoming the strong coupling between multiple parameters in the optimization process of the mechanism, and obtaining the ideal working trajectory and motion posture of transplanting. Xu et al.[12] improved the second-order gear combination by using the non-circular gears and spatial staggered helical gears combined transmission mode, so that the end trajectory of the transplanting arm produces lateral offset, realizing the transplanting of rice in wide and narrow rows. Jiang et al.[13] used a top-down parameter-driven design approach to effectively improve the uprightness of garlic potting seedlings.

The second-order non-circular planetary gear train and rod assembly combination mechanism inverse design method is based on the known trajectory of the end point of the rod and the motion posture of the end rod to inversely solve the key parameters of the mechanism. It can avoid the blindness of forward design, and the design accuracy is strong, which can obtain a more ideal motion trajectory and posture[14,15]. Zhao et al.[16] established an inverse design model of non-circular gears and obtained a combination of structural parameters of the mechanism to satisfy the trajectory by bionizing the static trajectory of rice potting and transplanting motion. Chen et al.[17] established an inverse design model with motion trajectory as the target and developed an inverse design software for transplanting mechanism. The influence of key points on the trajectory on the posture of the end transplanting nozzle was further analyzed to optimize the mechanism parameters and effectively reduce the seedling injury rate. Wu et al.[2] obtained better mechanism parameters and satisfied better transplantation posture requirements by forward design combined with inverse fine-tuning through localized inverse kinematic modeling. Wang et al.[18] established a spatial inverse design model and analyzed the influence of the angular difference of the cyclic motion of the mechanism components on the trajectory of the end point, so as to obtain the combination of the key parameters of the mechanism to satisfy the spatial transplantation motion.

In order to solve the problem of sugarcane, which is always difficult to meet the agronomic requirements for fixed-posture seeding, this paper is based on the second-order non-circular planetary gear system pendulum-type seeding mechanism, and pre-plans the key position and posture of the end-point motion of the seeding arm. Taking the initial position of the double-motion point of the rotation center of the intermediate non-circular gear and the rotation center of the planetary non-circular gear as the design parameter, the reverse optimization design model is established based on the motion law of the mechanism. The combination of key structural parameters is optimally solved by a genetic algorithm so that the mechanism meets the pre-planned requirements of multiple approximate positions and postures. This study establishes the inverse design model of the free pitch curve of non-circular gear and calculates the convexity value of each non-circular gear. In order to enhance the overall smoothness of the mechanism, a two-stage non-circular gear pitch curve optimization model is established with the motion angle of the rod assembly as the optimization parameter, and the optimal parameter combinations are screened in order to obtain the non-circular gear pitch curves with optimal roundness. Finally, the end point trajectory, posture, and non-circular gear pitch curve of the mechanism satisfy the design requirements.

2 Analysis of trajectory and posture of end point of seeding arm of sugarcane seeding mechanism

In order to meet the agronomic requirements of sugarcane seeding, it is necessary to ensure that the position and posture of the cane seeds show stable periodic changes with the movement of the seeding mechanism. After the posture recognition by the industrial camera, the cane seeds are transported to the designated point by the conveyor belt, and then the redirecting jaws will hold the cane seeds and transport them to the seed-picking point, so as to make them have a stable posture. The seeding mechanism then grips the cane seeds and carries out periodic seeding operations along the trajectory of movement. To facilitate the analysis of sugarcane seeding motion, the motion of the end point where the mechanism grips the cane seed is divided into the seed-picking section *ab*, seed-transporting section *bc*, seeding section *cd*, and return section *da*. The seeding arm picks up the seed at pickup point *a* and drops the seed at seeding point *d*. The seeding operation moves cyclically along a static trajectory of *abcda*. The static trajectory of the whole motion cycle is in the shape of an "8", and with the movement of the locomotive, the corresponding dynamic trajectory is formed (Figure 1). Throughout the entire cycle of seeding operations, the

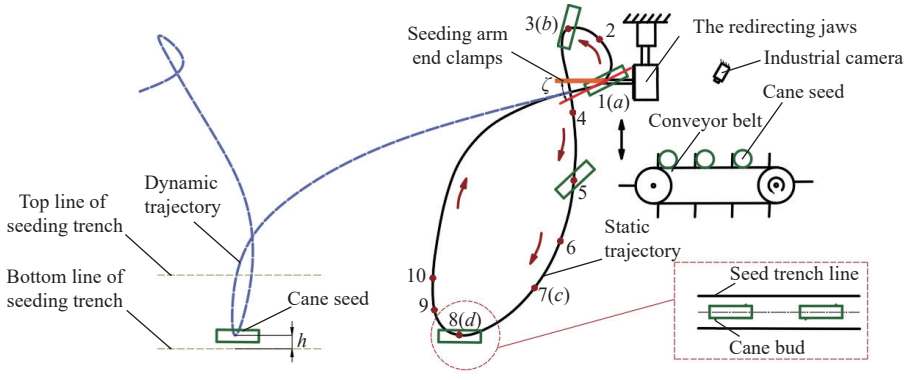

Figure 1 Schematic diagram of sugarcane seeding movement trajectory and selection of type-value points

following conditions need to be met: (i) The vertical distance between the seed transportation point b and the seed pickup point a is more than 120 mm, and the horizontal distance is more than 60 mm. (ii) The vertical distance between the seeding point d and the seeding point a is more than 550 mm, and the horizontal distance is more than 300 mm. (iii) At the seed-taking point a, the seeding arm is parallel to the axis of the redirecting jaws, and the angle with the cane axis (seed taking angle ζ) is greater than 25° and less than 30°. (iv) At the seeding point d, the axis of the cane seed is kept parallel to the axis of the seed trench, and the distance h of the cane seed from the bottom of the seed trench is more than 30 mm and less than 60 mm.

Based on the above requirements, 10 type-value points are pre-selected from the ideal trajectory under the premise of meeting the approximation requirements of the optimal design of the seeding mechanism. As far as possible, the posture of the seeding arm gripping the cane seeds at multiple key positions throughout the motion cycle is reasonably constrained in order to facilitate the comprehensive study of the approximate multi-position and posture of this seeding mechanism and to carry out the inverse optimization design.

3 Synthesis of approximate multi-position and posture motions of a sugarcane seeding mechanism

3.1 Principle of operation of the seeding mechanism

As shown in Figure 2, the second-order non-circular planetary carrier pendulum seeding mechanism uses a single planetary carrier in combination with two pairs of non-circular gears to drive the seeding arm for sequential seeding operation of the cane seeds. The sun gear 1 is fixed to the frame, and the intermediate non-circular gear 2 meshes with the sun gear 1 and drives coaxially with the intermediate non-circular gear 3, so that the intermediate non-circular gear 2 and the sun gear 1 can be regarded as the first stage of non-circular gears. The planetary non-circular gear 4 meshes with the intermediate non-circular gear 3 to drive and is solidly connected to the seeding arm 6, so that the planetary non-circular gear 4 and the intermediate non-circular gear 3 can be regarded as a second-stage non-circular gear. When the planetary carrier rotates clockwise at a uniform speed during operation, the intermediate non-circular gear 2 and the intermediate non-circular gear 3 rotate clockwise with respect to the planetary carrier and rotate clockwise with respect to the sun gear; the planetary non-circular gear 4 rotates counterclockwise with respect to the planetary carrier and rotates clockwise with respect to the sun gear. Due to the constraints on the degrees of freedom imposed by the planetary gear train, the seeding arm 6 moves periodically with the planetary carrier, and its end point p forms the trajectory of this seeding mechanism.

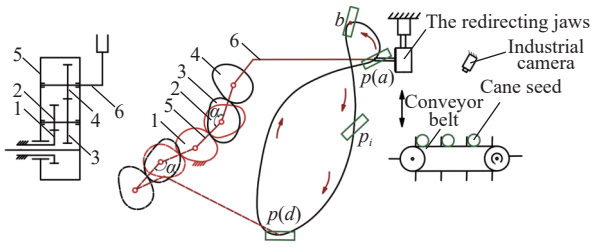

Figure 2 Schematic diagram of a pendulum seeding mechanism with a second-order non-circular planetary gear train

3.2 Approximate multi-position and posture motion analysis

The absolute motion of the planetary gear slewing center in line with the end point of the mechanism is a periodic reciprocating oscillation, the length of which can be regarded as the equivalent rod length of the seeding arm 6. The center of rotation of the sun gear 1 in line with the center of rotation of the planetary non-circular gear 4 is equivalent to a planetary carrier. Due to the existence of the offset angle α of the planetary carrier affecting the installation position of the intermediate noncircular gears, the entire second-order noncircular planetary gear train pendulum rod seeding mechanism was simplified to a planar open-chain 2R mechanism (Figure 3), where o is the center of rotation of the planetary carrier and a coordinate system is established with this point as the origin, A_i is the center of rotation of the intermediate non-circular gear, and B_i is the center of rotation of the planetary non-circular gear 4.

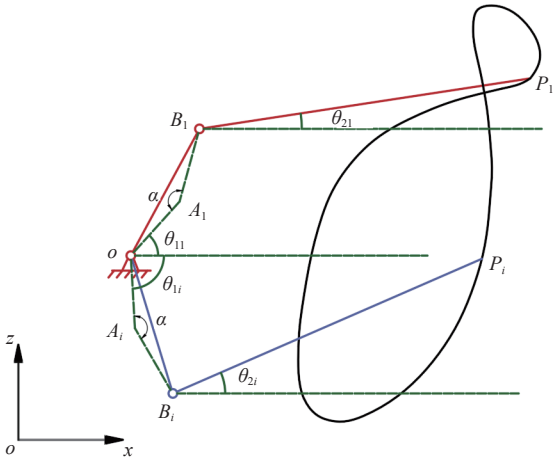

Figure 3 Schematic diagram of planar open-chain 2R mechanism

The approximate multi-position and posture motion is required to satisfy that the seeding arm end point p_i (x_{pi}, y_{pi}) (i=1, 2, ..., 10) passes sequentially through a given set of positions in the analyzed space and conforms to the corresponding posture requirements[19]. Let the angle between the planetary carrier and the horizontal line be θ_{1i} and the initial value be θ_{11}. Let the angle between the seeding arm and the horizontal line be θ_{2i} and the initial value be θ_{21}. Then the position transformation relation of the end point of this open-chain 2R mechanism from the 1st point to the i-th point in Figure 1 is:

$$\begin{pmatrix} x_{Bi} \\ y_{Bi} \\ z_{Bi} \end{pmatrix} = \begin{pmatrix} \cos\delta_i & -\sin\delta_i & x_{pi} - x_{p1}\cos\delta_i + y_{p1}\sin\delta_i \\ \sin\delta_i & \cos\delta_i & y_{pi} - x_{p1}\sin\delta_i - y_{p1}\sin\delta_i \\ 0 & 0 & 1 \end{pmatrix} \begin{pmatrix} x_{B1} \\ y_{B1} \\ 1 \end{pmatrix} \tag{1}$$

$$\begin{pmatrix} x_{Ai} \\ y_{Ai} \\ z_{Ai} \end{pmatrix} = \begin{pmatrix} \cos\varphi_i & -\sin\varphi_i & x_{Bi} - x_{B1}\cos\varphi_i + y_{B1}\sin\varphi_i \\ \sin\varphi_i & \cos\varphi_i & y_{Bi} - x_{B1}\sin\varphi_i - y_{B1}\sin\varphi_i \\ 0 & 0 & 1 \end{pmatrix} \begin{pmatrix} x_{A1} \\ y_{A1} \\ 1 \end{pmatrix} \tag{2}$$

where, $\delta_i = \theta_{2i} - \theta_{21}$ and $\varphi_i = \theta_{1i} - \theta_{11}$.

The planetary uncircular gear rotation center B_1 (x_{B1}, y_{B1},1) and the intermediate uncircular gear rotation center A_1 (x_{A1}, y_{A1},1) at the initial position are the design variables. Although A_i and B_i of this seeding mechanism are double moving points in periodic motion, A_iB_i is the intermediate non-circular gear in the single planetary carrier meshing center distance with the planetary non-circular gear 4 always remains the same. Therefore, based on the principle of fixed center distance, it can be obtained:

$$c_{i1}x_{B1}^2 + c_{i2}x_{B1}x_{A1} + c_{i3}x_{B1}y_{A1} + c_{i4}x_{B1} + c_{i5}y_{B1}^2 + c_{i6}y_{B1}x_{A1} + c_{i7}y_{B1}y_{A1} + c_{i8}y_{B1} + c_{i9}x_{A1}^2 + c_{i10}x_{A1} + c_{i11}y_{A1}^2 + c_{i12}y_{A1} + c_{i13} = 0 \tag{3}$$

where

$$c_{i1}=c_{i5}=\cos^2\delta_i+\sin^2\delta_i-1$$

$$c_{i2}=c_{i7}=2-2\sin\varphi_i\sin\delta_i-2\cos\varphi_i\cos\delta_i$$

$$c_{i3}=2\cos\delta_i\sin\varphi_i-2\cos\varphi_i\sin\delta_i$$

$$c_{i4}=2x_{p1}\cos\delta_i-2x_{pi}\cos\delta_i+2y_{p1}\sin\delta_i-2y_{pi}\sin\delta_i-2x_{pi}\cos^2\delta_i-2x_{p1}\sin^2\delta_i+2x_{p1}\cos\varphi_i\cos\delta_i+2x_{p1}\cos\varphi_i\sin\delta_i-2y_{p1}\cos\delta_i\sin\varphi_i+2y_{p1}\cos\delta_i\sin\delta_i-2y_{pi}\cos\delta_i\sin\delta_i-2y_{p1}\sin\varphi_i\sin\delta_i$$

$$c_{i6}=2\cos\varphi_i\sin\delta_i-2\cos\delta_i\sin\varphi_i$$

$$c_{i8}=2y_{p1}\cos\delta_i-2y_{p1}\sin^2\delta_i-2y_{pi}\cos\delta_i-2x_{p1}\sin\delta_i+2x_{pi}\sin\delta_i-2y_{pi}\cos^2\delta_i+2x_{p1}\cos\varphi_i\cos\delta_i-2x_{p1}\cos\varphi_i\sin\delta_i-2y_{p1}\cos\delta_i\sin\varphi_i-2x_{p1}\cos\delta_i\sin\delta_i+2x_{pi}\cos\delta_i\sin\delta_i+2y_{p1}\sin\varphi_i\sin\delta_i$$

$$c_{i9}=c_{i11}=\cos^2\varphi_i+\sin^2\varphi_i-1$$

$$c_{i10}=2x_{pi}\cos\varphi_i-2x_{p1}\cos\varphi_i-2y_{p1}\sin\varphi_i+2y_{pi}\sin\varphi_i-2x_{p1}\cos^2\varphi_i+2y_{p1}\sin^2\varphi_i+2x_{pi}\cos\varphi_i\cos\delta_i-2x_{p1}\cos\varphi_i\sin\varphi_i+2y_{p1}\cos\varphi_i\sin\varphi_i-2y_{p1}\cos\varphi_i\sin\delta_i+2y_{pi}\cos\delta_i\sin\varphi_i+2x_{p1}\sin\varphi_i\sin\delta_i$$

$$c_{i12}=2y_{pi}\cos\varphi_i-2y_{p1}\cos\varphi_i+2x_{p1}\sin\varphi_i-2x_{pi}\sin\varphi_i-2x_{p1}\cos^2\varphi_i-2y_{p1}\sin^2\varphi_i+2y_{pi}\cos\varphi_i\cos\delta_i+2x_{p1}\cos\varphi_i\sin\varphi_i+2y_{p1}\cos\varphi_i\sin\varphi_i+2x_{p1}\cos\varphi_i\sin\delta_i-2x_{pi}\cos\delta_i\sin\varphi_i+2y_{p1}\sin\varphi_i\sin\delta_i$$

$$c_{i13}=2x_{p1}^2\cos^2\varphi_i-2x_{p1}^2\cos\varphi_i\sin\delta_i+2x_{p1}^2\cos\varphi_i+x_{p1}^2\sin^2\delta_i+x_{p1}^2-2x_{p1}x_{pi}\cos\varphi_i\cos\delta_i-2x_{p1}x_{pi}\cos\varphi_i-2x_{p1}x_{pi}\cos\delta_i-2x_{p1}x_{pi}-4x_{p1}y_{p1}\cos\varphi_i\sin\varphi_i+2x_{p1}y_{p1}\cos\varphi_i\sin\delta_i+2x_{p1}y_{p1}\cos\varphi_i+2x_{p1}y_{p1}\sin\varphi_i\sin\delta_i-2x_{p1}y_{p1}\sin\varphi_i-2x_{p1}y_{p1}\cos\varphi_i\cos\delta_i-2x_{p1}y_{pi}\cos\varphi_i+2x_{p1}y_{pi}\cos\delta_i\sin\delta_i+2x_{p1}y_{pi}\sin\delta_i+x_{pi}^2\cos^2\delta_i+2x_{pi}^2\cos\delta_i+x_{pi}^2+2x_{pi}y_{p1}\cos\delta_i\sin\varphi_i-2x_{pi}y_{p1}\cos\delta_i\sin\delta_i+2x_{pi}y_{p1}\sin\varphi_i-2x_{pi}y_{p1}\sin\delta_i+2y_{p1}^2\sin^2\varphi_i-2y_{p1}^2\sin\varphi_i\sin\delta_i-2y_{p1}^2\sin\varphi_i+y_{p1}^2\sin^2\delta_i+y_{p1}^2+2y_{p1}y_{pi}\cos\delta_i\sin\varphi_i-2y_{p1}y_{pi}\cos\delta_i+2y_{p1}y_{pi}\sin\varphi_i-2y_{p1}y_{pi}+y_{pi}^2\cos^2\delta_i+2y_{pi}^2\cos\delta_i+y_{pi}^2$$

The system of equations can be further developed if this seeding mechanism is to clamp the sequence of cane seeds through the given N type-value points and satisfy the posture requirements at each position:

$$\begin{cases} f_2=c_{21}x_{B1}^2+c_{22}x_{B1}x_{A1}+c_{23}x_{B1}y_{A1}+c_{24}x_{B1}+c_{25}y_{B1}^2+c_{26}y_{B1}x_{A1}+c_{27}y_{B1}y_{A1}+c_{28}y_{B1}+c_{29}x_{A1}^2+c_{210}x_{A1}+c_{211}y_{A1}^2+c_{212}y_{A1}+c_{213} \\ f_3=c_{31}x_{B1}^2+c_{32}x_{B1}x_{A1}+c_{33}x_{B1}y_{A1}+c_{34}x_{B1}+c_{35}y_{B1}^2+c_{36}y_{B1}x_{A1}+c_{37}y_{B1}y_{A1}+c_{38}y_{B1}+c_{39}x_{A1}^2+c_{310}x_{A1}+c_{311}y_{A1}^2+c_{312}y_{A1}+c_{313} \\ \vdots \\ f_N=c_{N1}x_{B1}^2+c_{N2}x_{B1}x_{A1}+c_{N3}x_{B1}y_{A1}+c_{N4}x_{B1}+c_{N5}y_{B1}^2+c_{N6}y_{B1}x_{A1}+c_{N7}y_{B1}y_{A1}+c_{N8}y_{B1}+c_{N9}x_{A1}^2+c_{N10}x_{A1}+c_{N11}y_{A1}^2+c_{N12}y_{A1}+c_{N13} \end{cases} \tag{4}$$

Equation (4) contains the four set design variables x_{A1}, y_{A1}, x_{B1}, y_{B1} with N-1 independent equations. If N=5, the structural parameters of the open-chain 2R mechanism satisfying the exact multi-position and posture can be solved. There are nine independent equations in Equation (4) if N>5, i.e., the mechanism has to comply with the posture requirements for 10 type-value points. Therefore, the design variables of the four mechanisms solved only satisfy the approximate posture requirements at each type-value point. Then, based on Equation (4), a single-objective nonlinear optimization function can be further constructed as follows:

$$F(x_{A1},y_{A1},x_{B1},y_{B1})=\min\left(\sum_{j=2}^{N}f_j^2(x_{A1},y_{A1},x_{B1},y_{B1})\right) \tag{5}$$

Genetic algorithm with strong search capability and fast convergence speed can solve the combination of design variable parameters of the open-chain 2R mechanism corresponding to the minimum value of Equation (5). Based on the output parameters, an equivalent rod length L_1 of the planetary carrier, an equivalent rod length L_2 of the seeding arm, a center distance a_1 of the meshing of the sun gear with the intermediate non-circular gear 2, a center distance a_2 of the meshing of the intermediate non-circular gear 3 with the planetary non-circular gear 4, and a bias angle α of the planetary carrier in the final open-chain 2R mechanism can be obtained. The relationship between each structural parameter and the design variables is:

$$\begin{cases} L_1=\sqrt{x_{B1}^2+y_{B1}^2} \\ L_2=\sqrt{\left(x_{p1}-x_{B1}\right)^2+\left(y_{p1}-y_{B1}\right)^2} \\ a_1=\sqrt{x_{A1}^2+y_{A1}^2} \\ a_2=\sqrt{(x_{B1}-x_{A1})^2+(y_{B1}-y_{A1})^2} \\ \alpha=\arccos\dfrac{a_1^2+a_2^2-L_1^2}{2a_1a_2} \end{cases}$$

3.3 Solving the optimization model

Based on the agronomic requirements described in Section 1, the 10 type-value points on the trajectory shown in Figure 1 are planned, with the specific positions of the end points of the mechanism and the corresponding parameters of the mechanism's posture as listed in Table 1. Where the type-value point 1 coincides with the seed-taking point a, the type-value point 3 coincides with the seed transportation point b, and the type-value point 8 coincides with the seeding point d.

Table 1 Pre-planning type-value points and corresponding agency posture data

Type-value point	x_{pi}/ mm	y_{pi}/ mm	Planetary carrier posture angle θ_{1i}/(°)	Seeding arm posture angle θ_{2i}/(°)
1	618.2	300.9	43	10
2	642.4	374.8	17	32
3	555	437.2	–6	54
4	549.2	271.1	–45	47
5	560.2	131.1	–66	35
6	537.1	–36.2	–90	20
7	467.1	–182.0	–116	4
8	286.3	–303.2	–159	–18
9	220.8	–240.1	–183	–17
10	217.9	–161.9	–197	–14

Substituting the planned type-value points and posture data in Table 1 into Equations (4) and (5), the mounting positions of the

components of the seeding mechanism and the compactness of the structural design are considered. The boundary conditions for each design variable in the optimization function are set as:

$$\begin{cases} 70 \le x_{A1} \le 120 \\ 60 \le y_{A1} \le 110 \\ 150 \le \sqrt{x_{B1}^2 + y_{B1}^2} \le 350 \\ 100 \le \sqrt{(x_{B1} - x_{A1})^2 + (y_{B1} - y_{A1})^2} \le 160 \\ 400 \le \sqrt{(x_{P1} - x_{B1})^2 + (y_{P1} - y_{B1})^2} \le 600 \end{cases} \tag{6}$$

The effect of rounding error amplification due to data dimensionality is excluded, and genetic algorithms are used to minimize and iteratively optimize the established single-objective nonlinear optimization function[20]. The final fitness scatter plot is shown in Figure 4, which shows that the fitness function scatter tends to converge as the number of iterations increases. The design variables corresponding to the optimal values of the fitness function are: x_{A1}=90.8, x_{B1}=90.3, y_{A1}=132.3, y_{B1}=216.6. From this, the structural parameters of the open-chain 2R mechanism can be calculated as L_1=253 mm, L_2=497 mm, a_1=128 mm, a_2=132.5 mm, α=153°.

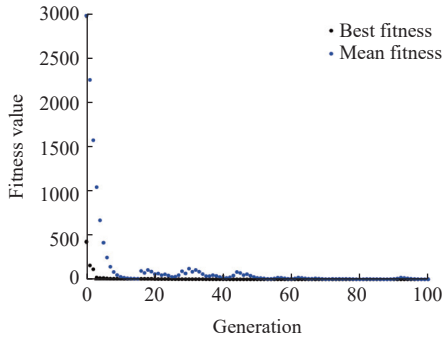

Figure 4 Scatterplot of optimal fitness

4 Design and optimization of non-circular planetary gear trains

4.1 Inverse design of non-circular gear pitch curves

According to the structural parameters of the open-chain 2R mechanism solved in Section 3.3 combined with the posture requirements of the mechanism when the end point p moves to different type-value points, the incremental change of the seeding arm with respect to the planetary carrier angle γ_i can be calculated when the planetary carrier angle change is φ_i.

$$\gamma_i = \theta_{2i} - \theta_{21} - (\theta_{1i} - \theta_{11}) \tag{7}$$

From Equation (7), the data in Table 1 were calculated and the relative angular displacement relationship curves (red solid points) of the open-chain 2R mechanism corresponding to the type-value points 1-10 were fitted using the 3-times non-uniform B-spline curves[21] (Figure 5). In order to obtain the relative angular displacement curve for the whole motion cycle, it is necessary to refer to the trajectory of the return segment and select three variable value points (blue solid points) based on the obtained structural parameters of the mechanism. Since the selected variable value point corresponds to the end point of the mechanism that has moved to the return section of the trajectory, the change of the selected value point only affects the shape of the trajectory and the posture of the seeding mechanism in part of the return section.

The absolute motion of the seeding arm is a synchronized reciprocating oscillation due to the planetary carrier driving the second-order non-circular gear planetary gear train in a periodic compound motion. Therefore, according to the geometrical motion relationship of the open-chain 2R mechanism, the total transmission ratio of this planetary gear train is:

$$i = \left| \frac{\omega_1}{\omega_2} \right| \tag{8}$$

where, ω_1 (°)is the angular velocity of rotation of the planetary carrier, and ω_2 (°)is the angular velocity of the seeding arm relative to the planetary carrier.

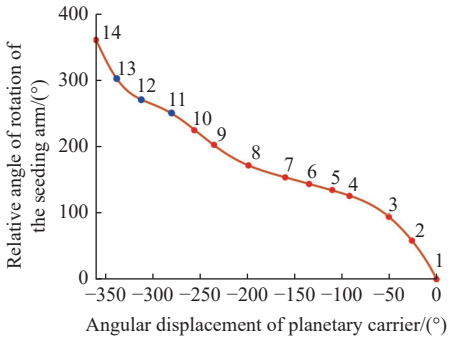

Figure 5 Relative angular displacement curve of seeding arm with respect to planetary carrier

In order to obtain the radius of the pitch curve of each non-circular gear in this planetary gear train, it is necessary to assign ratios to the non-circular gears of the two meshing stages. At the same time, in order to ensure the stability of the meshing transmission between the gears, it is necessary to make all levels of non-circular gear ratio approximation[22].

$$i = i_1 i_2 \tag{9}$$

where, i_1 is the ratio of the first non-circular gear, i_2 is the ratio of the second non-circular gear, and $i_1 = k_c \sqrt{i}$, k_c is the correction factor.

Therefore, the vectorial diameter of each gear in the second-order non-circular planetary gear train is:

$$\begin{cases} r_1(\varphi_i) = \dfrac{a_1}{1 + i_1(\varphi_i)}, \quad r_2(\varphi_i) = \dfrac{a_1 i_1(\varphi_i)}{1 + i_1(\varphi_i)} \\ r_3(\varphi_i) = \dfrac{a_2}{1 + i_2(\varphi_i)}, \quad r_4(\varphi_i) = \dfrac{a_1 i_2(\varphi_i)}{1 + i_2(\varphi_i)} \end{cases} \tag{10}$$

where, $r_1(\varphi_i)$, $r_2(\varphi_i)$, $r_3(\varphi_i)$, $r_4(\varphi_i)$ denote the radius of the pitch curves of the sun gear, the intermediate non-circular gear 2, the intermediate non-circular gear 3, and the planetary non-circular gear, respectively.

In order to obtain a pitch curve that meets the requirements of non-circular gear meshing transmission and to avoid sudden changes in the pitch curve, k_c = 0.9 is adjusted so that the peak position of the ratio curve of the non-circular gears at all levels is similar to the fluctuation trend of the total ratio. The total transmission ratio versus the ratio curves of the non-circular gears of each stage are shown in Figure 6. The pitch curves of the two pairs of non-circular gears solved based on the distribution of ratios are shown in Figure 7. From the pitch curve shape, the curvature variation of the non-circular gears is not uniform, and the overall smoothness needs to be further improved to facilitate the tooth profile design.

4.2 Determination of convexity of non-circular gears

The radius of curvature expresses the concavity of the pitch

curve of a closed free non-circular gear. If the radius of curvature at every point on the pitch curve of the non-circular gear is positive, it means that the non-circular gear does not have concavity[23]. In the polar coordinate system, the curve has a radius of curvature ρ:

$$\rho=\frac{\left[r^2+\left(\frac{dr}{d\varphi}\right)^2\right]^{\frac{3}{2}}}{r^2+2\left(\frac{dr}{d\varphi}\right)^2-\frac{rd^2r}{d\varphi^2}} \tag{11}$$

where, r (mm)is the radius of the pitch curve of the non-circular gear, and φ (°) is the rotation angle of the active gear during the transmission of a pair of non-circular gears.

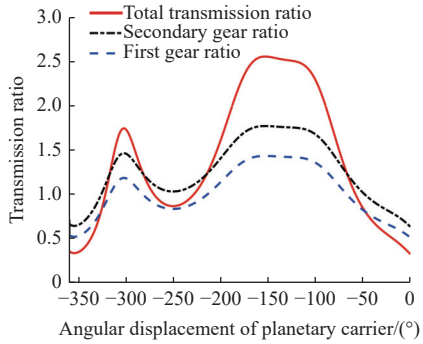

Figure 6 Ratio curves of non-circular gears of each stage

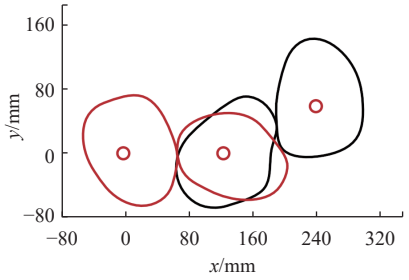

Figure 7 Non-circular planetary gear train pitch curve diagrams

Since the sun gear is always fixed to the frame during the working process of the mechanism, combined with the working principle of Section 3.1, for a first-stage non-circular gear meshing transmission, the rotation angle of the active gear is the rotation angle of the planetary carrier. Thus when the planetary carrier is rotated by an angle φ, for the sun gear 1:

$$\begin{cases}\dfrac{dr_1}{d\varphi}=\dfrac{a_1i_1'}{(1+i_1)^2}\\ \dfrac{d^2r_1}{d\varphi^2}=-a_1\dfrac{(1+i_1)i_1''-2i_1'^2}{(1+i_1)^3}\end{cases} \tag{12}$$

where, i_1' is the derivative function of the ratio curve of the first-stage non-circular gear, and i_1'' is its second-order derivative function.

Substituting Equation (12) into Equation (11) yields a radius of curvature function about the sun gear 1:

$$\rho_1=\frac{a_1\left[1+\left(\frac{i_1'}{1+i_1}\right)^2\right]^{\frac{3}{2}}}{1+i_1+i_1''} \tag{13}$$

Therefore, $q_1=1+i_1+i_1''$ can be considered as the convex value of the sun gear 1.

Let the intermediate non-circular gear 2 rotate by $\beta 2$ angle when the planetary carrier rotates by φ angle, so for the intermediate non-circular gear 2:

$$\begin{cases}\dfrac{dr_2}{d\beta_2}=\dfrac{dr_2}{d\varphi}\cdot\dfrac{d\varphi}{d_{\beta 2}}=\dfrac{a_1i_1'i_1}{(1+i_1)^2}\\ \dfrac{d^2r_2}{d\beta_2^2}=a_1i_1\dfrac{\left(i_1''i_1+i_1'^2\right)(1+i_1)-2i_1'^2i_1}{(1+i_1)^3}\end{cases} \tag{14}$$

where, $d\varphi/d\beta_2=i_1$.

Substituting Equation (14) into Equation (11) yields a radius of curvature function about the intermediate non-circular gear 2:

$$\rho_2=\frac{a_1i_1\left[1+\left(\frac{i_1'}{1+i_1}\right)^2\right]^{\frac{3}{2}}}{1+i_1+i_1'^2-i_1''i_1} \tag{15}$$

Therefore, $q_2=1+i_1+i_1'^2-i_1''i_1$ can be considered as the convexity value of the intermediate uncircular gear 2.

Let the angle of rotation of the intermediate non-circular gear 3 be β_3 when the planetary carrier turns through an angle φ. Since the intermediate non-circular gear 3 is coaxially driven with the intermediate non-circular gear 2, $\beta_3=\beta_2$. Therefore, for the intermediate non-circular gear 3:

$$\begin{cases}\dfrac{dr_3}{d\beta_3}=\dfrac{dr_3}{d\varphi}\cdot\dfrac{d\varphi}{d\beta_3}=\dfrac{-a_2i_2'i_1}{(1+i_2)^2}\\ \dfrac{d^2r_3}{d\beta_3^2}=-a_2i_1\dfrac{\left(i_2''i_1+i_2'i_1'\right)(1+i_2)-2i_2'^2i_1}{(1+i_2)^3}\end{cases} \tag{16}$$

where, i_2' is the derivative function of the ratio curve of the first-stage non-circular gear, and i_2'' is its second-order derivative function.

Substituting Equation (16) into Equation (11) yields a radius of curvature function with respect to the intermediate non-circular gear 3:

$$\rho_3=\frac{a_2\left[1+\left(\frac{i_2'i_1}{1+i^2}\right)^2\right]^{\frac{3}{2}}}{1+i_2+i_2''i_1^2+i_2'i_1'i_1} \tag{17}$$

Therefore, $q_3=1+i_2+i_2''i_1^2+i_2'i_1'i_1$ can be considered as the convexity value of the intermediate non-circular gear 3.

It is set that when the planetary carrier rotates by φ angle, the planetary non-circular gear 4 rotates by β_4 angle, so for the planetary non-circular gear 4:

$$\begin{cases}\dfrac{dr_4}{d\beta_4}=\dfrac{dr_4}{d\varphi}\cdot\dfrac{d\varphi}{d\beta_3}\cdot\dfrac{d\beta_3}{d\beta_4}=\dfrac{a_2i_2'i_1i_2}{(1+i_2)^2}\\ \dfrac{d^2r_4}{d\varphi_3^2}=a_2i_1i_2\dfrac{\left[\left(i_1'i_2+i_1i_2'\right)i_2'+i_2''i_1i_2\right](1+i_2)-2i_2'^2i_1i_2}{(1+i_2)^3}\end{cases} \tag{18}$$

Substituting Equation (18) into Equation (11) yields a radius of curvature function with respect to the planetary non-circular gear 4:

$$\rho_4=\frac{a_2i_2\left[1+\left(\frac{i_2'i_1}{1+i_2}\right)^2\right]^{\frac{3}{2}}}{1+i_2+i_2'^2i_1^2-i_1'i_2'i_1i_2-i_2''i_1^2i_2} \tag{19}$$

Therefore, $q_4=1+i_2+i_2'^2i_1^2-i_1'i_2'i_1i_2-i_2''i_1^2i_2$ can be considered as the convexity value of the planetary non-circular gear 4.

In the above equation, q_1, q_2, q_3, q_4 are all variables describing the state of local concavity and convexity of the pitch curve. If the value of convexity at a certain point is larger, it means that the point (and the nearby very small intervals) is locally more outwardly convex. When the convexity value is negative, it indicates that the pitch curve of the non-circular gear has a tendency to concave inward, which is unfavorable to the meshing transmission between non-circular gears. If the convexity value is greater than 3, it will lead to a larger amplitude of ratio change between meshing non-

circular gears, which is unfavorable to the stability of the non-circular planetary gear train transmission, thus affecting the unequal speed movement of the seeding mechanism[24].

4.3 Convexity optimization of pitch curves for non-circular planetary gear trains

Through the ratio curves of all levels of non-circular gears (Figure 6), the non-circular gear pitch curves that do not meet the requirements of the convexity value are calculated and searched, and it is determined that the sun gear 1 and the intermediate non-circular gear 2 convexity value is large; the maximum can be up to 3.203 and 3.106, respectively. The intermediate non-circular gear 3 appears to have a negative convexity value, with a minimum convexity value of –1.962. Based on the backward extrapolation of the non-compliant partial pitch curves to the section of the curve corresponding to the relative angular displacements, the relative angular displacement curve fitting is diversified at that stage, since the curve corresponds to the return section of the mechanism motion on which three variable value points are not fully defined. Optimization of non-circular gear convexity can be achieved by adjusting the blue solid variable value points on the relative angular displacement curve shown in Figure 5. Therefore, it is necessary to establish the optimization objective function of pitch curves between non-circular gears, and at the same time, the horizontal coordinates of the blue solid variable-valued points can be defined as the optimization variables. The conditions that need to be satisfied among the variables are:

$$\lambda_{10} \le x_{11} \le x_{12} \le x_{13} \le \lambda_{14}$$

where, x_{11}, x_{12}, and x_{13} are the horizontal coordinates of the variable value points on the relative angular displacement curve, and λ_{10} and λ_{14} are the horizontal coordinates of the fixed value points.

The three variable value points can be corresponded to points on the corresponding pitch curves of each non-circular gear, thus establishing a pitch curve radius difference function with nearby points, which can be used as a pitch curve optimization function. The first-stage non-circular gear optimization function is expressed as:

$$Y_1 = \sum_{k}^{M} \left(|r_{1(k+20)} - r_{1k}| + |r_{1(k-20)} - r_{1k}| + |r_{1(k+20)} - r_{2k}| + |r_{2(k-20)} - r_{2k}| \right) \tag{20}$$

where, r_{1k} and r_{2k} denote the radius values of the kth point on the pitch curves of the sun gear 1 and the intermediate non-circular gear 2, respectively; $r_{1(k+20)}$ and $r_{1(k-20)}$ are the radius values of the points near the kth point on either side of the sun gear 1; $r_{2(k+20)}$ and $r_{2(k-20)}$ are the radius values of the points near the kth point on either side of the intermediate noncircular gear 2.

Since the planetary non-circular gear 4 and the planetary non-circular gear 3 are meshing transmissions with fixed center pitch, the effect of the optimization of the pitch curve of the intermediate non-circular gear 3 on the pitch curve of the planetary non-circular gear 4 also needs to be taken into account when establishing the optimization function of the secondary non-circular gear. The secondary non-circular gear optimization function is expressed as:

$$Y_2 = \sum_{t}^{M} \left(|r_{3(t+20)} - r_{3t}| + |r_{3(t-20)} - r_{3t}| + |r_{4(t+20)} - r_{4t}| + |r_{4(t-20)} - r_{4t}| \right) \tag{21}$$

where, r_{3t} and r_{4t} denote the radius value of the t-th point on the pitch curves of the intermediate non-circular gear 3 and intermediate non-circular gear 4, respectively; $r_{3(t+20)}$ and $r_{3(t-20)}$ are the radius values of the points near the t-th point on either side of the intermediate noncircular gear 3; $r_{4(t+20)}$ and $r_{4(t-20)}$ are the radius values of the points near the t-th point on both sides of the planetary non-circular gear 4.

In order to fully and adequately evaluate the design solutions for each non-circular gear, multi-objective optimization of the above two optimization functions is required. Multi-objective genetic algorithm (NSGA)[25] has strong self-adaptation and optimization ability, which can be used to solve the complex pitch curve optimization problem of non-circular planetary gear train. In order to make the pitch curve convexity of each non-circular gear meet the requirements, the *NSGA* II algorithm is used to perform multi-objective optimization in order to output the optimal order solution set, and the data results are screened by entropy weight TOPSIS [26] combined with game theory.

After several optimization tests, the first-order non-circular gear pitch curve optimization weight coefficient of 0.6866 and the second-order non-circular gear pitch curve optimization weight coefficient of 0.3134 are obtained. The final output set of screened optimal order solutions is listed in Table 2, and the optimized set of optimal solutions for the Pareto front with screened optimal order solutions is shown in Figure 8.

Table 2 Optimization results of angular displacement parameters

Parameters	x_{11}	x_{12}	x_{13}
Upper value	–256	–256	–256
Lower value	–360	–360	–360
Optimum value	–268.1315	–289.7336	–321.1071

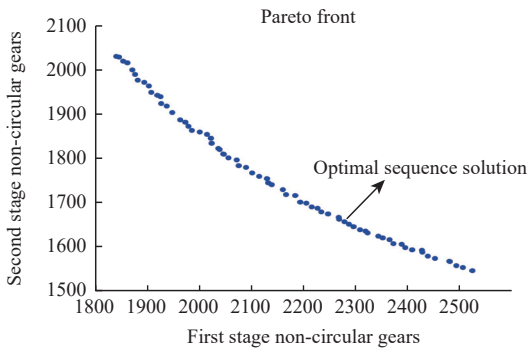

Figure 8 Optimal solution set of Pareto front for multi-objective parameter optimization

After a number of optimization screenings, the optimal value of the optimization function for the first-stage non-circular gear is obtained as 2278.87, and the optimal value of the optimization function for the second-stage non-circular gear is obtained as 1656.34. The relative angular displacement change curves before and after optimization are shown in Figure 9, and the non-circular gear pitch curves deduced based on the optimization are shown in Figure 10. Compared to Figure 7, it is clearly visible that the optimized non-circular gear pitch curves at all levels have more uniform curvature changes, the roundness becomes better, and the concavity and convexity of the non-circular gear pitch curves are obviously improved.

Based on the optimized pitch curves of non-circular gears at all levels combined with the parameters of the components that have been solved inversely, the seeding mechanism is subjected to a

recurrence analysis, and the final recurrence trajectory obtained is shown in Figure 11. Part of the trajectory in the return section has changed significantly, but since this part of the trajectory is in the variable trajectory section and the seeding mechanism is empty stroke, it will not affect the overall seeding operation.

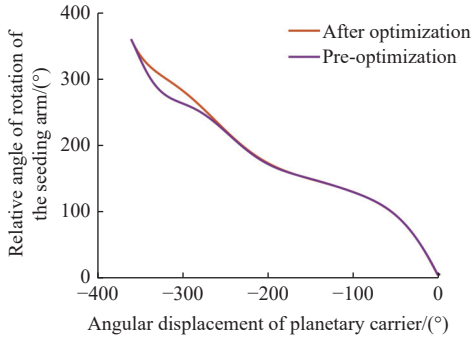

Figure 9 Relative angular displacement curves before and after optimization

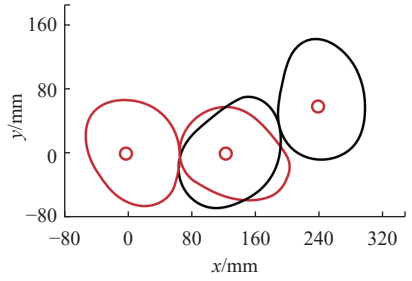

Figure 10 Optimized non-circular gear pitch curves

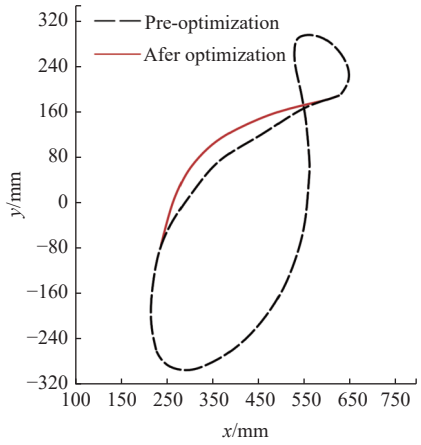

Figure 11 Trajectory changes before and after optimization

5 Simulation verification of the seeding mechanism

According to the inverse optimization design of the seeding mechanism and the multi-objective optimization of the pitch curves of the non-circular gears at all levels in Sections 3 and 4, the design and optimization parameters are modeled in three dimensions and the motion constraints of each component are added by Adams. The rotation speed of the planetary carrier is set to 180°/s, the simulation time is 2 s, and the motion trajectory obtained from the simulation is shown in Figure 12. The simulation results prove that the motion trajectory of the seeding mechanism and the posture of the seeding arm at the key position are basically consistent with the theoretical analysis. After measuring the virtual simulation results, the total error rate of calculating the posture of the seeding arm is 3.7113%, which indicates the correctness of the inverse optimization design method of the two-stage planetary gear train pendulum seeding mechanism with the theory of multi-objective optimization and screening of non-circular gear pitch curves.

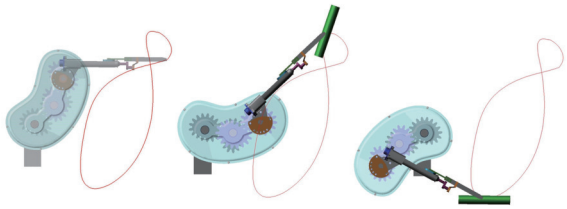

Figure 12 Kinematics of pendulum seeding mechanism with two-stage non-circular planetary gear train

6 Conclusions

(1) Since the current sugarcane planter cannot make the cane seeds accomplish complex sowing motion trajectories and postures, it does not meet the sowing agronomic requirements. An inverse optimization design method for approximate multi-position and posture of a pendulum seeding mechanism with second-order non-circular planetary gear train is proposed. By simplifying the complex seeding mechanism and based on pre-planning the 10 key positions and postures of the end point of the seeding arm, the inverse optimization design model of the double moving point of this mechanism is established. Combined with the genetic algorithm, the key double-motion point rotation center position of the mechanism is solved, and then the key structural parameters can be obtained. The design blindness of forward solving can be avoided by using an inverse optimization design scheme.

(2) By analyzing the motion law of the seeding mechanism, the fitted relative angular displacement curve, solving and reasonably allocating the transmission ratio of the second-order non-circular planetary gear train in order to establish the inverse design model of non-circular gear pitch curves at all levels. The convexity of each non-circular gear is modeled to determine whether the pitch curve of each non-circular gear meets the requirements of meshing transmission. The variable value points on the relative angular displacement curve are used as optimization parameters to establish the convexity optimization model of the non-circular gear pitch curve. Parameter optimization based on multi-objective *NSGA* II, combined with the entropy-weighted *TOPSIS* method in the set of Pareto frontier solutions, determined the preferred optimal combination of parameters for angular displacement optimization. The results show that the radius of curvature of the optimized and screened non-circular gear pitch curves change more uniformly and have better roundness.

(3) Based on Adams, this seeding mechanism is simulated and verified, and the simulation results show that its motion trajectory and the posture of the seeding arm at the key position are basically consistent with the pre-planned posture information and theoretical analysis. The motion error rate is 3.7113%, which meets the requirements of the complex motion trajectory and posture of the cane seed during the seeding motion. This proves the correctness and rationality of the optimization theory of the inverse optimal design of sugarcane seeding mechanism based on approximate multi-position and posture with the convexity of the pitch curve of the second-order non-circular gear.

Acknowledgements

This research work was supported by The National Natural Science Foundation of China (Grant No. 52265028), Guangxi

Natural Science Foundation of China (Grant No. 2021JJA160046), and Innovation Project of Guangxi Graduate Education (Grant No. YCSW2023362).

[References]

[1] Ou Y G, Wegener M, Yang D T, Liu Q T, Zheng D K, Wang M M, et al. Mechanization technology: The key to sugarcane production in China. Int J Agric & Biol Eng, 2023; 6(1): 1–27.

[2] Zhu Z F, Wu G H, Ye B L, Zhang Y C. Reverse design and tests of vegetable plug seedling pick-up mechanism of planetary gear train with non-circular gears. Int J Agric & Biol Eng, 2023; 16(2): 96–102.

[3] Xu H C, Wang L, Miao Y J, Sun L. Kinematic synthesis and optimization design of a rice pot seedling transplanting mechanism. Proceedings of the Institution of Mechanical Engineers, Part C: Journal of Mechanical Engineering Science, 2024; 238(5): 1366–1381.

[4] Sun L, Huang X W, Xu Y D, Ye Z Z, Wu C Y. Automation creation method for a double planet carrier gear train transplanting mechanism based on functional constraints. Mech Sci, 2022; 13(1): 543–558.

[5] Cheng B, Wu H R, Zhu H J, Liang J, Miao Y S, Cui Y L, et al. Current status and analysis of key technologies in automatic transplanters for vegetables in China. Agriculture, 2024; 14(12): 2168.

[6] Yu G H. Study on vegetable plug seedling pick-up mechanism of planetary gear train with ellipse gears and incomplete non-circular gear. Journal of Mechanical Engineering, 2012; 48(13): 032.

[7] Xu C L, Lv Z J, Xin L, Zhao Y. Optimization design and experiment of full-automatic strawberry potted seedling transplanting mechanism. Transactions of the CSAM, 2019; 50(8): 97–106. (in Chinese)

[8] Liu J D, Cao W B, Tian D Y, Tang H Y, Zhao H Z. Kinematic analysis and experiment of planetary five-bar planting mechanism for zero-speed transplanting on mulch film. Int J Agric & Biol Eng, 2016; 9(4): 84–91.

[9] Zhou M L, Yang J J, Yin J J, Wang Z L. Design method and experimental study of a rice transplanting mechanism with three planting arms constrained by differential noncircular gear trains. Journal of the ASABE, 2022; 65(2): 221–233.

[10] Sun L, Wang Z F, Wu C Y, Zhang G F. Novel approach for planetary gear train dimensional synthesis through kinematic mapping. Proc. Inst. Mech. Eng. Part C-J. Eng. Mech. Eng. Sci., 2020; 234(1): 273–288.

[11] Ma G X, Mao H P, Han L H, Liu Y, Gao F. Reciprocating mechanism for whole row automatic seedling picking and dropping on a transplanter. Applied Engineering in Agriculture, 2020; 36(5): 751–766.

[12] Xu Y D, Zhu Y H, Xue X L, Wang L, Sun L, Yu G H. Optimal design and experiment on gear train wide and narrow row transplanting mechanism of spatial direct extraction and large offset of ratooning rice. Transactions of the CSAM, 2022; 53(9): 83–90. (in Chinese)

[13] Sun W, Feng J, Jiang Y Y. Optimal design and experiment of vertically transplanting mechanism with non-circular gears system for garlic (*Allium Sativum* L). Transactions of the CSAM, 2020; 51(8): 73–82. (in Chinese)

[14] Tong Z P, Yu G H, Zhao X, Liu P F, Ye B L. Design of vegetable pot seedling pick-up mechanism with planetary gear train. Chinese Journal of Mechanical Engineering, 2020; 33(1): 11.

[15] Wang L, Sun L, Yu G H, Zhou Y Z. Approximate motion generation of an epicyclic gear train with noncircular gears based on optimization–homotopy algorithm. Journal of Mechanisms and Robotics, 2023; 15(4): 041002.

[16] Zhao X, Chu M Y, Ma X X, Dai L, Ye B L, Chen J N. Research on design method of non-circular planetary gear train transplanting mechanism based on precise poses and trajectory optimization. Advances in Mechanical Engineering, 2018; 10(12): 1–12.

[17] Zhao X, Ye J, Chu M Y, Dai L, Chen J N. Automatic scallion seedling feeding mechanism with an asymmetrical high-order transmission gear train. Chinese Journal of Mechanical Engineering, 2020; 33: 1–14.

[18] Wang L, Sun L, Huang H M, Yu Y X, Yu G H. Design of clamping-pot-type planetary gear train transplanting mechanism for rice wide-narrow-row planting. Int J Agric & Biol Eng, 2021; 14(2): 62–71.

[19] Sun L, Hu Y X, Xing Z Q, Yu G H, Yu Y X. Motion synthesis of rotary pot seedling transplanting mechanism based on approximate multi-pose. Transactions of the CSAM, 2020; 51(12): 103–111. (in Chinese)

[20] Wang L, Sun L, Xu Y D, Yu G H, Gervais N L. Multi-pose motion synthesis of three-arm gear train planting mechanism based on genetic algorithm. Transactions of the CSAM, 2022; 53(6): 70–77. (in Chinese)

[21] Chung K-L, Yan W-M. A fast algorithm for cubic b-spline curve-fitting. Comput Graph, 1994; 18(3): 327–334.

[22] Yu G H, Tong Z, Sun L, Tong J, Zhao X. Novel gear transmission mechanism with twice unequal amplitude transmission ratio. Journal of Mechanical Design, 2019; 141(9): 092304.

[23] Ao M, Yu G H, Wang L, Sun L, Zhao J. Optimization synthesis of hybrid six-bar mechanism with non-circular gear constraints. Journal of Mechanical Design, 2023; 145(6): 064502.

[24] Sun L, Xu Y D, Huang H M, Wang Z F, Zhang G F, Wu C Y. Solution and analysis of transplanting mechanism with planetary gear train based on convexity of pitch curve. Transactions of the CSAM, 2018; 49(12): 83–92. (in Chinese)

[25] Shokri A, Bozorg-Haddad O, Marino M A. Algorithm for increasing the speed of evolutionary optimization and its accuracy in multi-objective problems. Water Resour. Manag, 2013; 27(7): 2231–2249.

[26] Jahanshahloo G R, Lotfi F H, Izadikhah M. An algorithmic method to extend TOPSIS for decision-making problems with interval data. App.Math Comput, 2006; 175(2): 1375–1384.